LIDAR STUDIES OF OZONE

V.V. Zuev, V.E. Zuev, and V.N. Marichev

Institute of Atmospheric Optics,
Siberian Branch of the Russian Academy of Sciences, Tomsk
Received June 16, 1993

In this paper we make an overview of papers presented at the 16th ILRC (Massachusetts, USA, July 20–24, 1992) and devoted to studies of the tropospheric and stratospheric ozone. Basic peculiarity of observations of the atmospheric ozone during this time is the influence of Mt. Pinatubo eruptive cloud of aerosols on the ozone content and on the reconstruction of ozone profiles.

Sixteen papers devoted to laser sounding of ozone in the atmosphere were presented at the 16th International Laser Radar Conference (ILRC). Nine of them discussed the problem of volcanic aerosol in the stratosphere with respect to both aerosol and ozone interaction and aerosol component consideration when measuring the ozone profiles. Negative correlation between the ozone content and volcanic aerosol has been observed in the stratosphere. At the same time, their interactions should be examined at length. To correctly reconstruct the vertical ozone distribution (VOD) from data obtained with differential absorption lidars (DIAL) in the presence of volcanic aerosol layers in the stratosphere, it is proposed

– a technique of correcting the aerosol scattering at fundamental and reference wavelengths,

– a measurement technique that uses, in addition to DIAL observations, the channels for acquiring Raman scattering signals what allows one to avoid the difference in aerosol scattering.

In many of the experiments, simultaneous soundings of the ozone and aerosol were accomplished to study the ozone destruction and to improve the method for correcting the lidar data on ozone. To test reliability of lidar measurements of the ozone, the data from SAGE–II satellite, ECC and Brewer–Mast sondes, and Umkehr–spectrometers were used. The ozone concentration profiles measured with lidars and these instruments were in good agreement that enabled one to employ them in ozone studies and in reconstructing extended profiles covering the troposphere and the stratosphere.

Validity of the ozone measurement data in the lower stratosphere in the regions affected by Mt. Pinatubo eruption has been checked by Grant, Browell, et al. (Ref. 1) during the airborne Arctic Stratospheric Expedition (AASE–II). It was assumed that the correction for differential aerosol scattering, which is especially important in the presence of a large amount of volcanic aerosol, can be reliably made when the wavelengths of sounding radiation are close and the Bernoulli method is used to process the data.

The data on stratospheric ozone in the tropics obtained with an airborne DIAL were compared with the results obtained using other instruments. The SAGE–II spectrometer and the electrochemical cell on (ECC) sondes were used as reference devices. The single measurement accuracy for SAGE–II was 7–10% in the 15 to 50 km region and that for the ECC sonde was 5–8% in the 10 to 31 km region. Figure 1 depicts a comparison of SAGE–II data between 10°S and 10°N for April from 1985 till 1991 with ECC sonde values for the second quarter of 1991. The two sets of values well agree within 5 to 10% accuracy except for low altitudes where measurements were made in different air volumes.

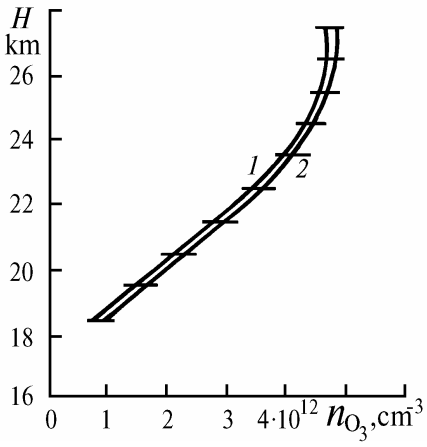

FIG. 1. A comparison of ECC sonde (curve 1) and SAGE–II (curve 2) stratospheric ozone measurements prior to the eruption of Mt. Pinatubo.

A similar comparison was made between SAGE–II data and UV–DIAL data on the ozone for a region unaffected by the Mt. Pinatubo volcanic aerosols (20°N to 25°N) (Fig. 2). Depicted to the right of the figure is the aerosol scattering ratio profile $R-1$. The DIAL values exceed the SAGE mean values by about one standard deviation, except at 18.5 km, where the aerosol loading was the greatest. The agreement between these data can be considered quite well if, again, one takes into account that different volumes of the atmosphere were observed by SAGE–II satellite and the lidar.

0235-6880/93/10 687-14 $02.00

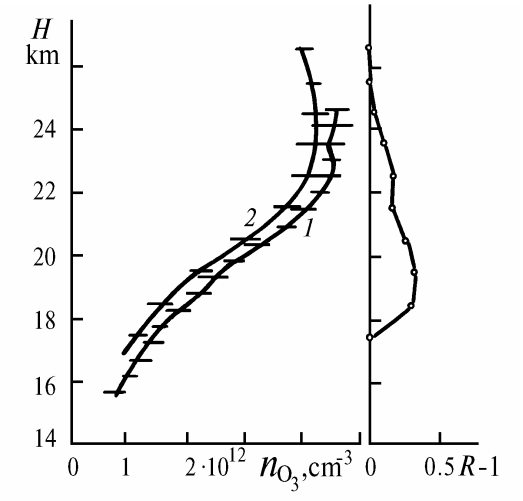

FIG. 2. A comparison of UV DIAL (January 30, 1992; curve 1) and SAGE–II (January and February, 1985–1991; curve 2) stratospheric ozone measurements in the region (20°N *to* 25°N) *unaffected by volcanic aerosols.*

The effect of aerosol from the Pinatubo volcano on the ozone content in the stratosphere is shown in Fig. 3. In this figure one can see the data on the ozone content measured during September–October periods in 1985–1990 from SAGE–II satellite and the data on the ozone content obtained in Brasil during the second half of 1991 with ECC sondes, the former data being considered as relating to the background ozone content. The reduction in ozone content as measured by sondes is significant (about 20%) in the altitude range from 20 to 27 km where the aerosol content is the highest and, the column density reduction being about 7%.

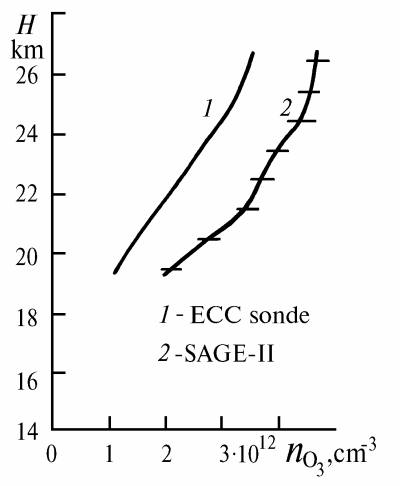

FIG. 3. Same as in Figure 1, but for the second half of 1991 (ECC–sonde data) and September–October periods of 1985–1990 (SAGE–II).

A comparison of stratospheric ozone measurement data (Fig. 4) obtained with SAGE–II in January 1985–1991 in the region 10°N to 15°N (background ozone concentrations) and data obtained with UV DIAL lidar in January 30, 1992 in the region 10°N to 14°N reveals a significant reduction in ozone concentration similar to that measured by ECC sondes.

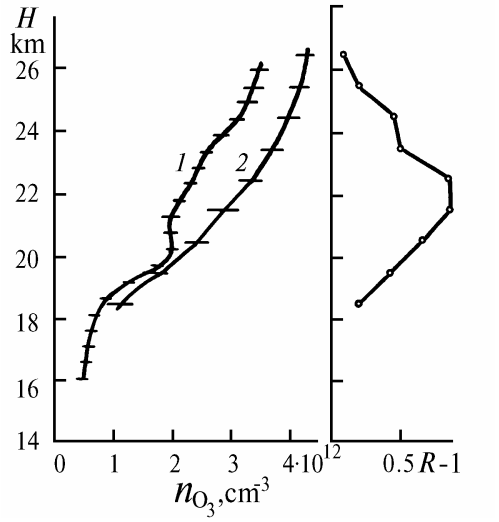

FIG. 4. Same as in Fig. 2, but for a region strongly affected by Mt. Pinatubo volcanic aerosols. Depicted to the right is the aerosol scattering ratio profile R–1.

Thus the complex observations show good agreement between the SAGE–II, ECC–sonde, and UV DIAL lidar measurements in the absence of Mt. Pinatubo aerosols and between the latter two in the presence of the Mt. Pinatubo eruptive cloud of aerosol. Therefore the UV DIAL lidar can be used to investigate the relationship between the ozone concentration and aerosol loading and their stratification as well.

An intercomparison experiment for different DIAL lidar systems used for sounding tropospheric ozone was undertaken in the period from June 10 till June 28, 1991 in the Netherlands within the framework of the European environmental research program EUROTRAC (TROLIX–91 campaign) (Ref. 2). The main scientific goals of the TROLIX–91 campaign were

– to compare the LIDAR measurements to *in situ* measurements of the ozone concentration,

– to determine the number of wavelengths, sounding at which would provide accurate reconstruction of the ozone profile in the low troposphere under realistic conditions,

– to assess the accuracy that can be achieved under realistic conditions,

– to compare the performance characteristics of the systems used in the campaign.

Four different UV DIAL systems involved in the campaign, used sounding radiation at different wavelengths from 248 to 313 nm. Two of the lidars (RIVM and CNRS/SA) used Nd:YAG laser and the third one used a KrF excimer laser. In all of these three lidars stimulated Raman shifting in H_2 and D_2 was employed. The fourth system (LIT) used a dye laser pumped with a Nd:YAG laser. The lidar measurements were accompanied by ground–based observations as well as by radiosonde soundings (temperature and humidity profiles) from a nearby meteorological station.

In order to avoid possible interference of the effect of spatially inhomogeneous aerosol on the ozone observations in the UV the intercomparison measurements have been carried out with all the lidars looking upward from one and the same measurement site. Moreover, reference measurements have also been carried out with a UV

photometer and ECC sondes from a heliciopter flying over this same site.

Then the experiments were continued along a horizontal path close to a long path of a differential optical absorption spectrometer (DOAS). Preliminary results showed that under certain favorable conditions a good agreement between data acquired with different systems was observed even at a high enough spatial resolution. Some negative effects, like sensitivity to steep gradients in aerosol concentration and interference with SO_2, were also studied in detail. The whole set of thus collected data enabled the assessment of these effects.

Steinbrecht and Carswell[3] proposed a technique of accounting and correcting the DIAL measurements of the ozone concentration for interference of Mt. Pinatubo aerosol. It was used for processing of the data obtained by the scientific group at York University in Toronto, Canada (42.80°N, 79.50°W, 200 m) with a lidar based on a XeCl laser, since March 1991. The expression for the ozone concentration, n_{O_3} obtained by the DIAL technique is written as:

$$n_{O_3}(H) = \frac{1}{2\Delta\sigma_{O_3}}\left\{\frac{d}{dH}\ln\frac{P(H,\lambda_{off})}{P(H,\lambda_{on})} - \frac{d}{dH}\ln\frac{\beta(H,\lambda_{off})}{\beta(H,\lambda_{on})}\right\} - \quad (a) \qquad (b)$$

$$- \frac{1}{\Delta\sigma_{O_3}}\left\{n_{Re}(H)\Delta\sigma_{Re} - \Delta\alpha_{Mie}(H)\right\}; \quad (1)$$
$$(c) \qquad (d)$$

$$\Delta\sigma_{O_3} = \sigma_{O_3}(\lambda_{on}) - \sigma_{O_3}(\lambda_{off});$$

$$\Delta\sigma_{Re} = \sigma_{Re}(\lambda_{on}) - \sigma_{Re}(\lambda_{off});$$

$$\Delta\alpha_{Mie} = \alpha_{Mie}(\lambda_{on}) - \alpha_{Mie}(\lambda_{off}).$$

Here σ_{O_3} and σ_{Re} are the cross sections of absorption by ozone and Rayleigh scattering, α_{Mie} is the aerosol extinction coefficient, $P(H)$ is the lidar return power as a function of height H, $\beta(H)$ is the backscattering coefficient, n_{Re} is the air molecule concentration, λ_{on} and λ_{off} are the on–line and off–line wavelengths of sounding radiation used for sounding the ozone.

When the aerosol content is negligible, β_{on}/β_{off} is constant and term (b) vanishes. The value $\Delta\alpha_{Mie}$ can also be neglected. The term (c) can easily be calculated using the atmospheric density profile. However, after a strong volcanic eruption, like that of Mt. Pinatubo, the terms (b) and (d) become quite important. In this case α and β must be calculated using Mie theory and balloon sonde measurements. The calculational results for β_{Mie} and α_{Mie}, assuming that aerosol is comprised of homogeneous spherical droplets of H_2SO_4 in water, are presented in Figs. 5 and 6. Calculations were done for 308, 353, 532, and 694 nm wavelengths and for four particle size–distributions corresponding to different layers at different times during July and August, 1991. Also shown in Fig. 5 is the β_{Mie} profile measured by lidars at 353 and 532 nm.

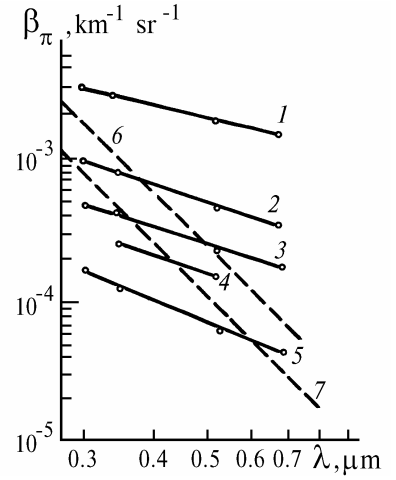

FIG. 5. Coefficients β_{Mie} calculated for four particle size–distributions. Curve 1 is for July 30, 1991, H = 23 km; *2 is for July 26, 1991,* 17 km; *3 is for August 8, 1991,* 22 km; *4 is for August 29, 1991,* 16.5 km; *and 5 is for August 29, 1991,* 16.5 km. *Aerosol layer at* 41°N *is shown by lines 1 – 3, 5; at* 44°N - *by line 4. The particle size–distribution is by Deshler et al. (CRL 19, 199–202, 1992). Lines 6 and 7 show the values β_{Re} at altitudes* 16.5 *and* 22 km, *respectively.*

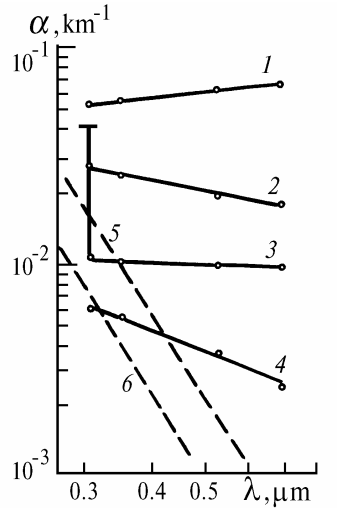

FIG. 6. Coefficients α_{Mie} calculated for four particle size–distributions. Curve 1 is for July 30, 1991, H = 23 km; *2 is for July 26, 1991,* 17 km; *3 is for August 29, 1991,* 22 km; *and 4 is for August 29, 1991,* 16.5 km. *The particle size–distribution is by Deshler et al. (CRL 19, 199–202, 1992). Lines 5 and 6 show the values α_{Re} at altitudes* 16.5 *and* 22 km, *respectively. Vertical line shows typical extinction profile due to absorption by ozone.*

If correcting the term (c) using known density profile (spectral dependence of the molecular scattering is λ^{-4}) one can reach 1–2% accuracy of correction. It is more difficult to estimate contribution to the error coming from terms (b) and (d). Figure 6 shows that $\Delta\alpha_{Mie}$ is too variable, because

of variations in the aerosol size spectra. The radiosonde–data–based correction can diminish the contribution to the total error coming from term (d) to 5 to 10 per cent while use of uncorrected value of the term (d) can yield a 50% error.

Taking into account the fact that $\beta(H, \lambda) = \beta_{Re} + \beta_{Mie}$ and using the law $\lambda^{-\eta}$ for Mie scattering (η is determined from the data in Fig. 5), the expression for the term (b) is written as

$$\frac{d}{dH} \ln \frac{\beta(H, \lambda_{off})}{\beta(H, \lambda_{on})} = \frac{(\lambda_{off}/\lambda_{on})^{\eta-4} - 1}{[1 + R^*(\lambda_{off}/\lambda_{on})^{\eta-4}][1 + R^*]} \times$$

$$\times \frac{d}{dH} R^*(H) = \varepsilon(H) , \qquad (2)$$

$$R^*(H) = \beta_{Mie}(H, \lambda_{off})/\beta_R(H, \lambda_{off}) .$$

The correction ε of the ozone concentration is shown in Fig. 7. The calculations were done for lidar measurements at 353 nm at the two individual nights. For comparison, a typical ozone profile is depicted in the figure. The index η varies within 1.1–1.8. The influence of η on the value (b) is seen to be negligible. The value of ε depends mostly on the slope of the profile R and its value and increases in the region of a bend. Ignorance of the term (b) leads to the error of 50% to over 100%. Numerical differentiation leads to significant errors in pronounced layers. Therefore it is advisable first to sum terms (a) and (b) and then perform the differentiation. On the whole, the correction for the influence of terms (b) and (d) could reduce the error of the ozone measurements to 10–20%.

An improved technique for processing of the DIAL data of stratospheric ozone sounding was proposed by Vandersee, Schönenborn, and Claude.[4] This approach allowed the authors to reconstruct vertical distribution of the ozone concentration from observational data obtained at the lidar station in Hohenpeissenberg up to 50 km altitude.

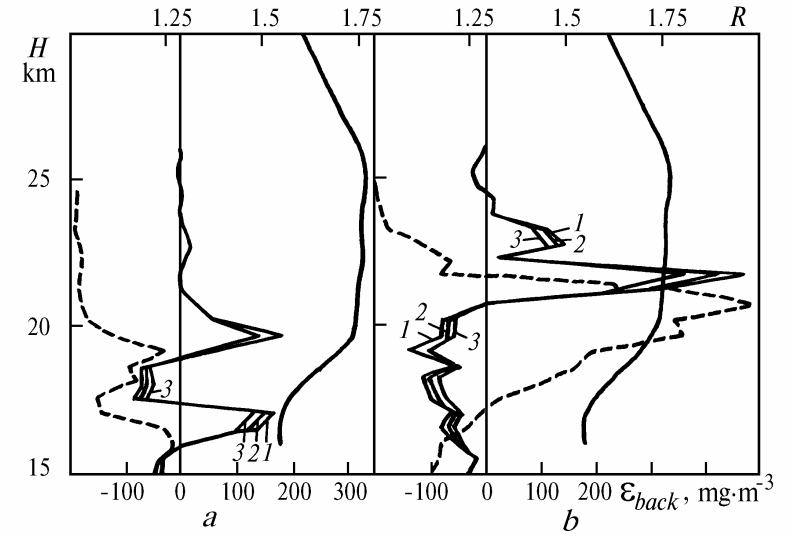

FIG. 7. Correction ε_{back} of the ozone concentration caused by the difference in backscattering coefficients for lidar measurements on August 21 (a) and October 23 (b), 1991. Calculations have been done for three values of η: η = 1.1 (1), 1.37 (2), and 1.8 (3). The profile of scattering ratio R (dashed line) and a typical ozone profile (solid line) are also shown for reference.

In this approach first the relative error in signal measurement is calculated for each height interval (time gate) assuming Poison statistics of photocounts, which is then used to estimate a resulting error according to Gaussian. After normalizing the signal by a number of shots and reducing it to vertical resolution of 1 km the signal profile is corrected for a PMT nonlinearity using an empirical function

$$S^*(I) = S(I) \, (a \exp (g(I - N_{min} + 1)) + 1) , \qquad (3)$$

where S^* is the actual number of photocounts, S is the recorded number of photocounts in channel I, N_{min} is the number of the lowest height interval involved into the processing procedure, and a is a constant;

$$g = b \, f \, (N_{min})^c , \qquad (4)$$

where b and c are constants, f is the count rate at the PMT output in the height interval, N_{min} in MHz (normally the maximum count rate value). The constants a, b, and c are found to be 0.5085, – 0.61274, and – 0.4771, respectively.

Equations (3) and (4) are valid for correcting signals recorded with an EMI 9893QB/350 PMT up to a maximum count rate of 12 MHz. Equations (3) and (4) show that nonlinear distortions of signals throughout the height channels depend on the maximum count rate at the PMT's output, i.e., the effect of nonlinearity increases with increasing maximum count rate. The measured (dotted) and corrected (solid line) lidar return profiles are shown in Fig. 8. It is seen from this figure that a larger maximum signal at a PMT's output results in a more rapid fall off of a lidar return that finally can cause overestimation (underestimation) of actual ozone concentration. The difference between vertical ozone distributions reconstructed with correction (solid line) and without correction (dotted line) can be seen in Fig. 9. The ozone profile obtained with the Brewer–Mast–sonde, also shown for a comparison in this figure, confirms the usefulness of this correction.

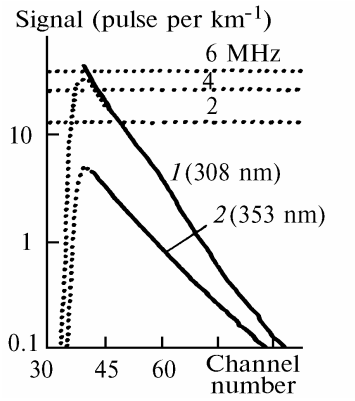

FIG. 8. Correction for a PMT nonlinearity.

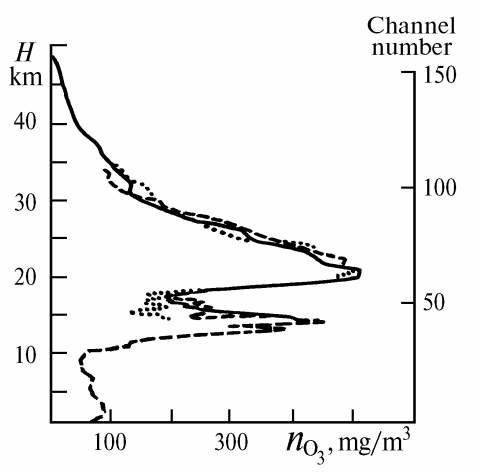

FIG. 9. Vertical ozone distribution measured by a lidar on March 7, 1991 (dotted line is for one hour of accumulation, solid line is for eight hours data accumulation) and Brewer–Mast sonde on March 1, 1991.

The next stage of lidar data processing involved filtration of the signal logarithms using a low–frequency Gaussian filter. The filter weight W_k was calculated by the expression

$$W_k = 1/\sqrt{2\pi}\,\exp\left(-\frac{k}{2}(\sigma/T^*)^2\right), \quad k = 1, 2, \ldots, \infty \qquad (5)$$

The series is truncated when $W_{k=n} < 0.1W_{k=1}$, where $W_{k=1}$ is the central channel weight, T^* is the desired filter efficiency determining the frequency spectrum of the lidar return fluctuations which must be removed.

$$T^* = A\,\exp\,(B(I - N_{\min} + 1) - C(I - N_{\min})^4), \qquad (6)$$

where A = const; $B = \ln(T^*_{\max}/A)\,4/(3\,I^*_{\max})$;

$$C = B/\,(4\,I^{*3}_{\max}). \qquad (7)$$

Since T^* increases exponentially with height, the error in the ozone estimation remains approximately constant, while the spatial resolution becomes poorer. To save a reasonable height resolution in the upper altitude range T^* is limited by $T^*_{\max}$ in the channel $I^*_{\max}$. Normally, in lidar measurements the integration time was between one and eight hours and $T^*_{\max} = 70$, what corresponds to a height resolution of 3.7 km. It is assumed that $T^* = T^*_{\max}$ for $I > I^*_{\max}$. As a result, the error in determining ozone content increases in this case. After filtering the value $\ln(S_{\text{off}}/S_{\text{on}})$ is calculated.

The temperature dependence of the absorption cross section and the Rayleigh scattering contribution were allowed for season averaged temperature and air density profiles which were obtained from radiosonde data for 1967 till 1986 period and which were extrapolated using standard atmosphere to altitudes above 32 km.

The above–described correction of lidar returns is quite sufficient for achieving better accuracy of measurements, except for situation when aerosol layers due to volcano eruptions occur in the stratosphere. A mechanical chopper was used to protect the photomultipliers against the overload. Therefore the photomultipliers worked far below the saturation limit so that all measurements were free of signal–induced noise.

The instrumental method of removing the aerosol effect on the ozone measurements by the differential absorption method in the UV and its application are discussed in several papers. The main idea of the method is in the use of Raman–lidar returns from molecular nitrogen what allows one to avoid the difference of aerosol scattering at two wavelengths of sounding radiation used for ozone sounding.

In Goddard Space Flight Center (NASA, USA) a mobile differential absorption lidar system operating based on Rayleigh and Raman light scattering was constructed. It makes it possible to carry out high–accuracy measurements of ozone concentration in the altitude range between 15 and 50 km (Ref. 5). The observations of the stratospheric ozone with this system have been made during February 1992 at the JPL–laboratory observation facilities (Table Mountain, California). The Rayleigh lidar returns at 308 and 351 nm, and corresponding Raman–lidar returns from N_2 at 332 and 382 nm were recorded. The product of atmospheric transitions at 351 and 382 nm wavelengths can be obtained from the Raman signal at 382 nm. Since the wavelength difference between 332 and 382 nm is nearly the same as that between 308 and 351 nm, the wavelength dependence of aerosol extinction is assumed to be the same for the wavelength pairs at 382 and 351 nm and at 308 and 332 nm. This information is then used in calculations of the ozone content. As the results of lidar measurements in February–March, 1992 show, the Raman scattering signals at lower altitudes and the Rayleigh ones at higher altitudes are sufficiently strong that makes it possible to obtain continuous profiles of ozone from 15 to 50 km.

A differential absorption lidar system for long–term measurements of stratospheric ozone was specially developed in the JPL laboratory and mounted on the Table Mountain (TMF–lidar, 34.4°N, 117.7°W).[6] This system is intended to be an element of an International network for detecting stratospheric changes (NDSC). The TMF–lidar has been tested in a number of intercomparisons, culminating in the first formal NDSC sponsored intercomparison – the Stratospheric Ozone Intercomparison Campaign 1989 (STOIC–89). A long series of measurement results obtained using different ozone profiling instruments has shown quite a satisfactory agreement (within about 5% accuracy) between the results provided that sounding conditions are the same or very close. Over the first four years of operation of the TMF lidar more than 450 profiles of ozone were acquired. They are fairly evenly distributed throughout the years and there is only a small increase in the number of

measurements during summertime. These results clearly show the existence of seasonal variations in the ozone profile. Variations of a monthly mean ozone content at 30 km altitude, are shown in Fig. 10. The monthly mean climatology of the ozone in this region is slightly different than that suggested by various model atmospheres, e.g. MAP model. The stratospheric aerosol layer from the Mt. Pinatubo eruption was first detected by the TMF lidar in July 1991. The effect of volcanic aerosol on the ozone measurement precision studied using the TMF and GSFC lidars was taken into account in the development of the DIAL–lidar for a new observatory at the Mauna Loa (MLO lidar). The MLO lidar has been additionally equipped with two Raman–lidar channels that provide for detecting Raman lidar returns from molecular nitrogen at 332 and 385 nm for correcting aerosol scattering. The MLO system used a 100 W, XeCl excimer laser, a new PC–based photon counter with 250 MHz maximum count rate, and a system of synchronization between all of the counting channels. The reference wavelength at 353 nm is generated by stimulated Raman scattering in hydrogen. The receiving telescope of a sufficiently high optical quality has the diameter larger than 1 m. The transmitting optics expands the laser beam by 5 times. A mechanical chopper used in this system provides for total cutting of the optical signal in 10 μs. The MLO system was planned to be put into operation in summer of 1992.

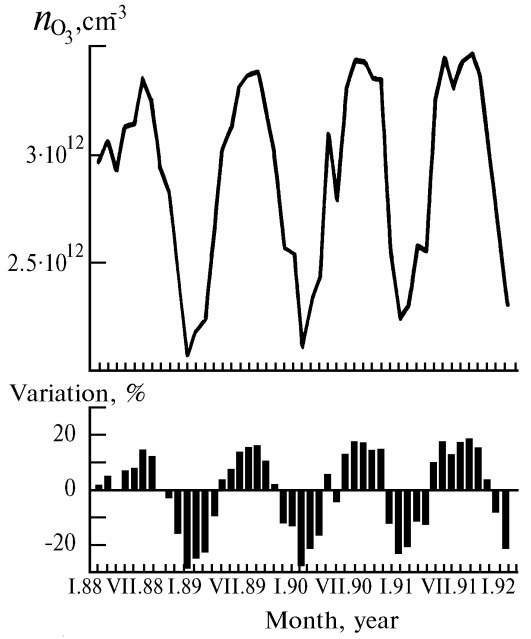

FIG. 10. Seasonal variations of the monthly mean ozone concentration at 30 km *altitude.*

Observation of the stratospheric ozone during 1988–1992 was made in Japan (Tsukuba, 36°N 140°E) (Ref. 7). The NIES lidar as an element of the Network for the Detection of Stratospheric Change (NDSC) enabled one to measure ozone and temperature profiles in the altitudes ranges 15 to 45 and 30 to 80 km, respectively. The lidar has a 2 m–diameter telescope, a XeCl (308 nm) and XeF (351 nm) excimer lasers. In 1991 the transmitter was additionally equipped with a KrF eximer laser (λ = 248 nm). Stimulated Raman scattering conversion is used in the system to generate some supplementary wavelengths: 339 nm from the XeCl–laser and 343 nm from the KrF–laser in D_2 cells (the 1st and 2nd Stokes components, respectively).

The ozone profiles were obtained using both pairs of sounding wavelengths 308–351 nm (*A*) and 308–339 nm (*B*). Agreement between ozone profiles obtained with *A* and *B* wavelength pairs was quite good until the stratospheric aerosol from the Mt. Pinatubo eruption arrived at Tsukuba. Typical ozone profiles obtained from the *A* and *B* wavelength pairs are shown in Fig. 11 and a temperature profile obtained from the 351 nm signal is shown in Fig. 12. Figure 13 presents a comparison made between the ozone profiles obtained with the NIES–lidar and SAGE–II satellite. Only insignificant disagreement takes place between individual and mean zonal profiles. Variations of the ozone content during 1988–1991 at 20, 25, 30, 35, and 40 km are depicted in Fig. 14.

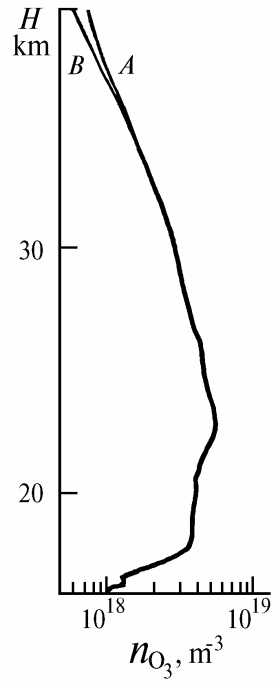

FIG. 11. Ozone profiles obtained with the NIES lidar on February 20, 1991.

Seasonal variations are easily seen in the ozone content at 20, 30, and 35 km heights which are qualitatively understood as a result of dynamic and photochemical effects. Systematic errors in the ozone profiles due to the effect of Mt. Pinatubo stratospheric aerosol are distinctly separated out from data of multiwavelength lidar measurements. In the ozone profiles obtained during the period when the largest value of scattering ratio *R* was observed (on February 26, 1992) (Fig. 15), it is possible to see a negative deviation of the ozone concentration, stronger one for (*A*) and weaker for (*B*) wavelength pair. This experimentally obtained wavelength dependence of the ozone profiles is proposed to be used for correcting sounding data for the influence of stratospheric aerosol.

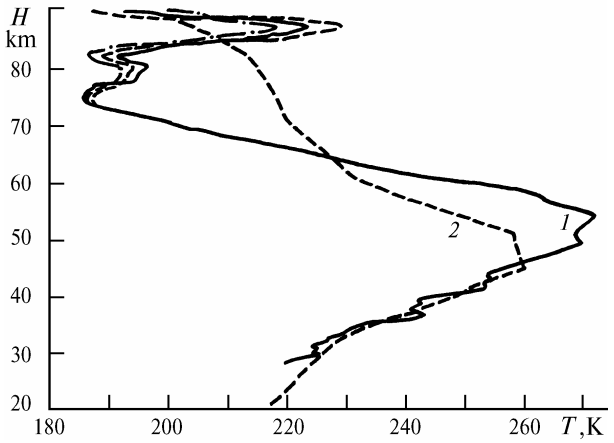

FIG. 12. A temperature profile observed with the NIES lidar on January 26, 1990 is shown by curve 1 and NASA model, 1988 - by curve 2.

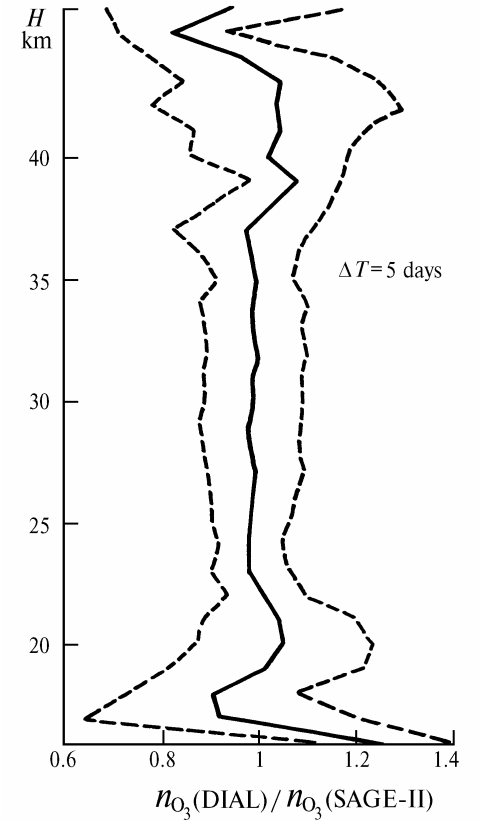

FIG. 13. Comparison of the ozone profiles obtained with the NIES ozone lidar and from SAGE–II measurement data. The figure shows the average ratio of lidar data to SACE–II data and the corridor of this ratio variations.

Measurements of the stratospheric ozone, temperature, and aerosol have also been conducted with the NASA/GSFC mobile stratospheric lidar during the UARS–92 Campaign at the JPL–laboratory facilities (Table Mountain).[8] Because of the presence of substantial amounts of residual volcanic aerosol from the Mt. Pinatubo eruptive cloud, the GSFC lidar system was modified by introducing of additional Raman scattering channel to provide more accurate ozone measurements. It enabled one, during strong aerosol overburden of the stratosphere, to obtain continuous profiles of ozone in the altitude range 15 to 50 km what was impossible in the previous measurements. The lidar was the only instrument capable of acquiring correct information about vertical ozone distribution in the lower stratosphere among the instrumentation employed in the UARS Campaign. Figure 16 shows three complete vertical profiles of the ozone from 15 to 50 km along with the appropriate MAP and US Standard models.

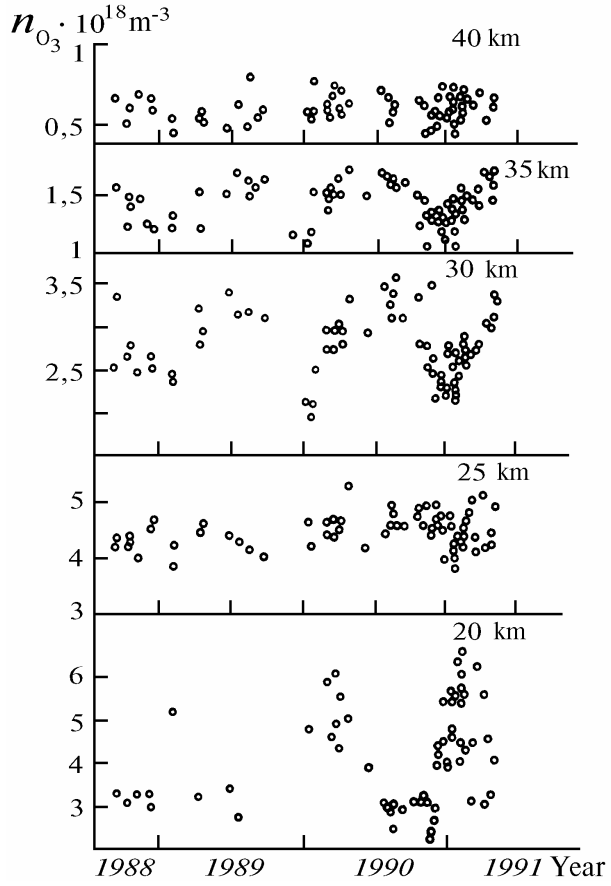

FIG. 14. Variations of the ozone content at 20, 25, 30, 35, *and* 40 km *altitudes as observed with NIES lidar.*

The temperature measurements were made using a XeF–laser (351 nm, 150 mJ/pulse, 70 Hz) in the altitude range 30 to 75 km. For acquiring enough accurate data on temperature profile 600000 shots were needed. The atmospheric density profile was calculated from the lidar returns at 351 nm. The temperature profile was computed for the derived relative density profile using the hydrostatic equation and the ideal gas law. Figure 17 depicts three vertical profiles of temperature for the same three nights as in Fig. 16. The temperature profiles are reconstructed from these data only down to 30 km height since the aerosol presence at lower altitudes does not allow to do this.

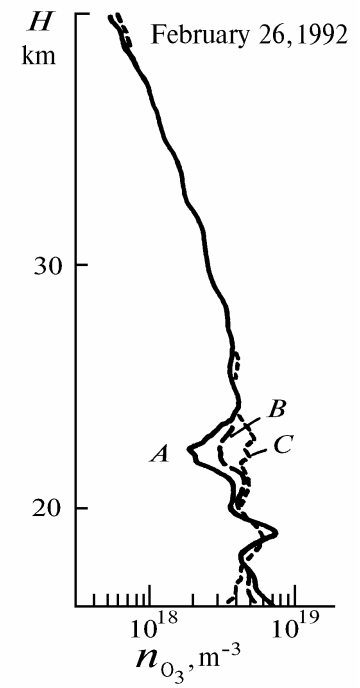

FIG. 15. Ozone profiles obtained from A, B, and C signal pairs. The peak of the Pinatubo aerosol layer was at about 20 km.

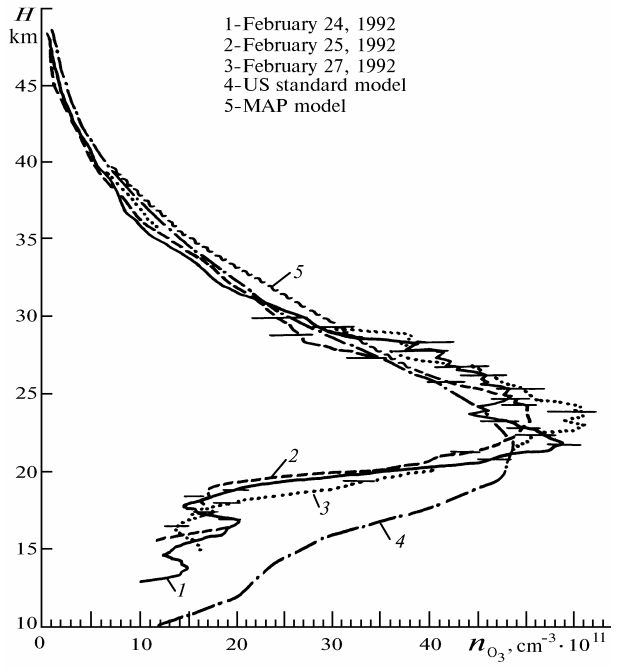

FIG. 16.

Simultaneous use of the Rayleign and Raman–lidar techniques allowed the measurements of both the aerosol scattering ratio R and extinction α in the stratosphere to be performed. The profiles of these obtained sounding data at 351 nm are shown in Figs. 18 and 19. These measurements were used to correct the low altitudes ozone profiles.

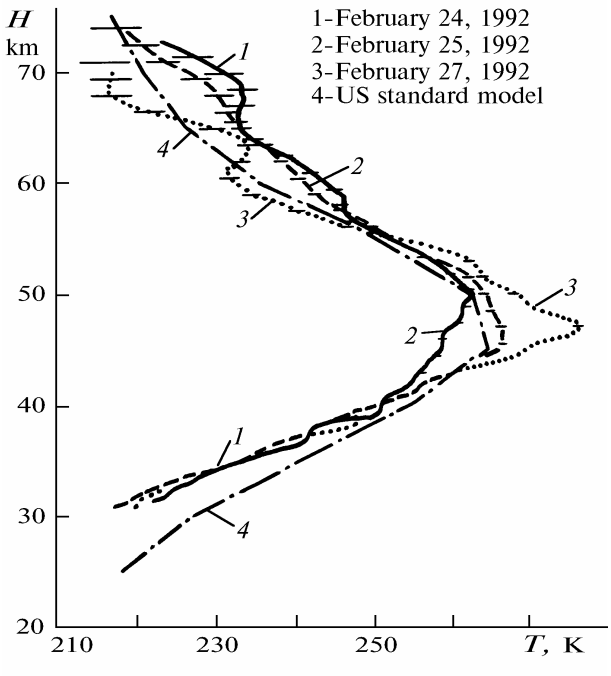

FIG. 17.

The lidar measurements of aerosol and ozone distributions in the stratosphere from January till March 1992 were made as part of the NASA Airborne Arctic Stratospheric Expedition[9] (AASE–II). The presence of Pinatubo volcanic aerosol in the stratosphere at that time caused the necessity of making corrections of the ozone measurements for the effect of aerosol light scattering. The correction for difference of aerosol backscatter in lidar returns at 301.5 and 310.87 nm was performed when solving the Bernoulli equation. In this case it is necessary to know the lidar ratio q and the index α^* in the spectral dependence of the aerosol backscatter at measured wavelengths. The parameter α^* can be determined directly from lidar returns in the infrared (1064 nm) and visible (603 nm) regions. Then the value α^* is extrapolated to the UV region. The value α^* can also be determined from a pair of signals 607 nm and λ_{off} after correcting the scattering ratio at λ_{off} for the absorption by ozone. The mean value of this parameter determined from measurements is $\overline{\alpha}^* = 0.7$. The value q is unknown *a priori*, but its variation only slightly affects the correction. A nominal value of $q = 0.028$ sr^{-1} was used in the calculations.

The sensitivity of the aerosol correction to the parameters α^* and q was investigated based on data obtained during two flights (AASE–II campaign) accomplished at two adjacent heights on January 30, 1992 over a region with geographical coordinates 20°N and 120°E. The first profile R (curve *1*, Fig. 20) was obtained during a 5 minute flight inside a strong aerosol layer from Mt. Pinatubo at 15 km altitude, then the profile R (curve *2*) was obtained outside the aerosol layer also during a 5 m flight. A comparison of the ozone profiles constructed using data of these flights without a correction for aerosol backscatter (Fig. 21) reveals their strong difference in the altitude region where large gradient of aerosol

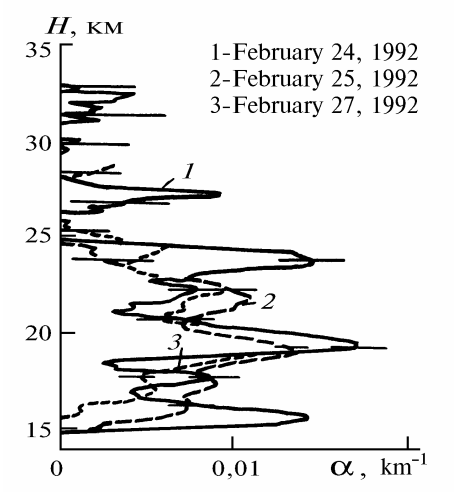

FIG. 18.

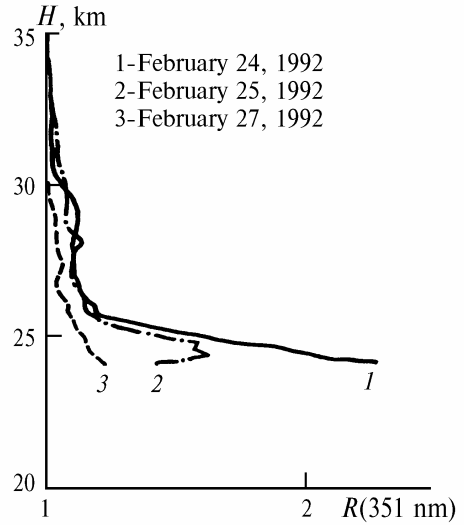

FIG. 19.

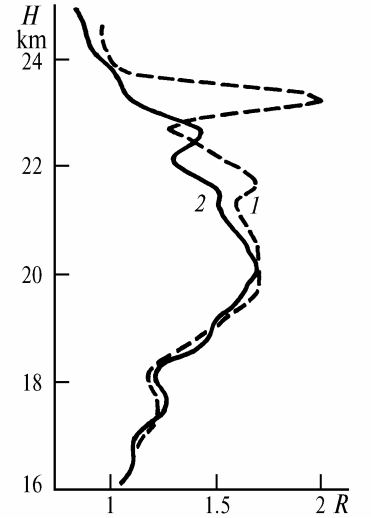

FIG. 20. Scattering ratio at λ_{off} (inside the layer (1) and outside it (2) derived from the Bernoulli equation. Vertical resolution of measurements is 525 m *at a horizontal averaging over 5 minutes flight line.*

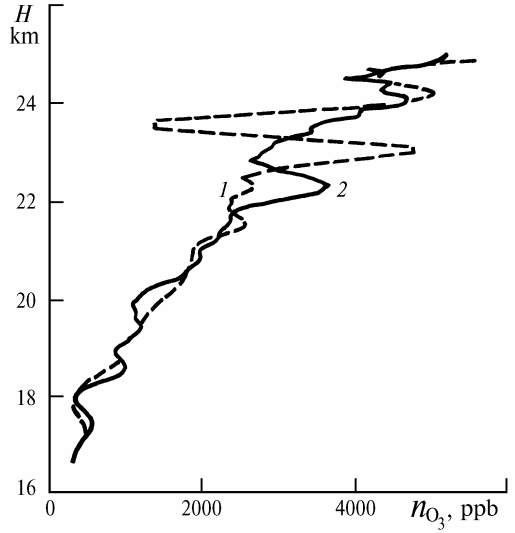

FIG. 21. Measured profiles of the ozone mixing ratio without a correction for the aerosol backscatter. Inside the layer (1) and outside it (2). The resolution is the same as in Fig. 20.

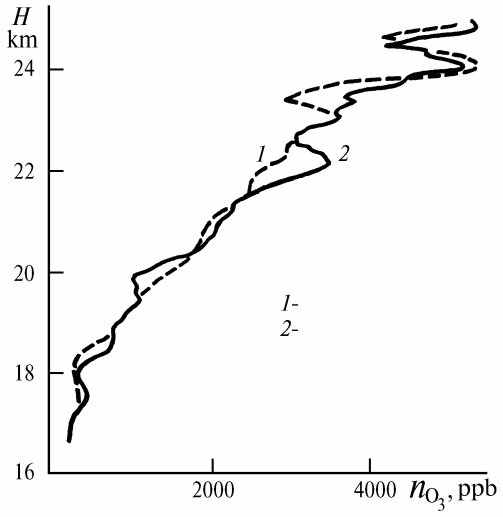

FIG. 22. Measured profiles of the ozone mixing ratio with a correction for the aerosol backscatter. Inside the layer (1) and outside it (2). The resolution is the same as in Fig. 20.

content occurs, i.e., at 23 km. The anomaly in the ozone vertical distribution coincides with the aerosol layer. Figure 22 shows the ozone profiles reconstructed from these same data but using the above – described correction and assuming that $\alpha^* = 0.7$ and $q = 0.028$. The ozone profiles are quite close to each other, but inside the layer the ozone concentration is 25% lower. This is interpreted as a real difference in the ozone contents inside and outside the aerosol layer rather than measurement error.

The flights accomplished from the pole to the equator allowed a vast experimental material to be compiled that, in turn, made it possible to reveal altitude regions in the stratosphere, where no correction for the aerosol backscatter was needed (clear air conditions, $R = 1$). Besides, the values α^* used in the corrections were also determined in these flights. This value can vary from flight to flight. Once it is assumed that the correction removes anomalous features, the remaining differences in the measured ozone profiles within aerosol–rich and aerosol–free regions are assumed to be actual differences in the ozone contents.

A combined airborne ozone and aerosol lidar was developed at the DLR laboratory of the Institute of Physics of the Atmosphere in Germany.[10] This lidar was constructed to measure two–dimensional ozone and aerosol fields in Arctic. The transmitter consists of two lasers: an excimer XeCl laser (λ = 308 nm, 250 mJ) and a Nd:YAG–laser (third harmonic, λ_{off} = 354 nm, 50 mJ) operating at 5 Hz frequency. The receiving optics consists of a 35 cm–diameter Cassegrainian telescope and of three optical channels arranged using color dividing dielectric coated beam splitters and filters. Lidar returns were recorded in an analog mode.

During the period from December 1991 till March 1992 46 flights of the summed duration of 300 hours were performed. The flights were accomplished from Sweden to Greenland, westwards (50°W) and to Novaya Zemlya, eastwards (60°E) and up to 85°N. By the end of March campaign, a north–south section was undertaken from 68°N to 17°N. The aerosol was measured almost all the time, the ozone was measured only under nighttime conditions. The vertical resolution was 1 km, an altitude range of measurements was from 13 to 25 km, and the flight height was 7 km. The horizontal resolution was between 50 to 200 km, depending on accuracy and range requirements. The lidar returns at λ_{on} and λ_{off} and the reconstructed ozone profiles are represented in Figs. 23 and 24.

Lidar measurements[11] of aerosol and ozone and their interaction have been made at the Observatoire de Haute–Provence (44°N, 5°E) since 1980. The system consists of several lidars, balloon sondes, and UV and visible spectrometers.

Routine measurements of the vertical distribution of backscattering coefficients from the tropopause up to 30 km, with an accuracy better than 10% and altitude resolution of 0.5 km were started in 1980. Since 1986 the routine measurements of the ozone in the stratosphere (15 to 48 km heights) are being carried out there and ozone profiling in the troposphere started in 1991. Two differential absorption lidars are used. The stratospheric lidar emitted at 308 (XeCl–laser) and 355 nm (third harmonic of the Nd:YAG laser). The tropospheric lidar emitted at 266 (fourth harmonic of the Nd:YAG laser) and 289–299 nm (stimulated Raman effect in H_2 and D_2 cells). The systems used an 80 cm–diameter receiving telescope and spectrometers to separate the backscattered radiation of different wavelengths. The lidar returns were recorded in analog and photon counting regimes (300 MHz).

The lidar data were compared with the ozone–sonde (Brewer–Mast and ECC–sondes) and Umkehr spectrometer data. More than 1000 Umkehr observations and 200 lidar profiles were included into the data base from 1985 till 1987. It was found from the data analysis that vertical profiles of the ozone reconstructed from data obtained using an updated Umkehr technique (it allows for temperature dependence of the absorption cross section) agree with the data of lidar measurements better. Thus, for example, in the layers 4 to 7 (at 20 to 38 km altitude) there is only insignificant disagreement between two methods (within the statistical error). In the layer 8 (H = 38–44 km) the agreement between the methods is mainly observed in winter months that can be accounted for by noise induced by lidar returns and large variability of temperature profiles during a day.

The aforementioned measurements make the basis for determining long–term trends in ozone vertical distribution, because the majority of ozone profiles compiled so far were obtained using the Umkehr technique. Similar comparisons with the SAGE–II data were also performed and showed a very good agreement between the satellite–borne system and the lidar measurements (within ± 2%, between 20 and 42 km heights).

Taking into account a large number of O_3 profiles already available from lidar measurements, studies of the natural variability of the ozone vertical distribution were undertaken which cover different temporal and spatial scales of variations. Seasonal variations of the stratospheric ozone were revealed from analysis of its annual cycle at the 30 km altitude. A half year cycle of ozone was revealed at higher altitudes. This fact confirms the importance of temperature dependent chemical processes in the upper stratosphere. In the troposphere, correlative studies of ozone and related meteorological characteristics, such as potential vorticity, geopotential, and relative humidity provide indication of the causes of the variability observed in the ozone vertical distribution. The intra–annual variations of the ozone content are shown to reflect the influence of the two main sources: the anthropogenically driven photochemical source and the dynamic source related to the stratosphere–troposphere exchange processes. Studies of such events including tropopause folds and low–altitude temperature inversions allow one to assess the inflow of stratospheric ozone to the troposphere as a result of dynamic processes. No evidence for an ozone trend in the troposphere between 1985 and 1991 can be noticed in the data of these measurements.

The measurements performed in 1991 following the major eruption of the Mt. Pinatubo volcano allowed one to follow the evolution of the volcanic cloud in the stratosphere over mid–latitude regions. Thus a limited increase in $R(H)$ at λ = 532 nm below 20 km was observed until mid October, 1991. Much larger values of $R(H)$ were observed at heights from 10 to 15 km at 532 nm that were related to the meridional transportation of the clouds. Simultaneous ozone measurements by the lidar, ozone–sonde and Dobson spectrometer

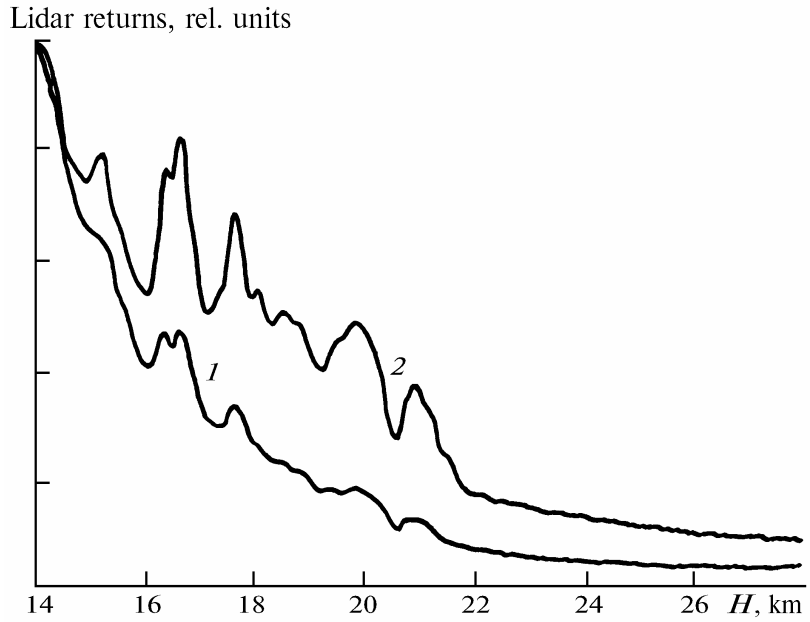

FIG. 23. The H^2–corrected lidar returns at the wavelengths 308 (λ_{on}, *curve 1) and* 354 nm (λ_{off}, *curve 2). The signals are averaged over* 1000 *laser shots (horizontal averaging over* 30 km *flight line).*

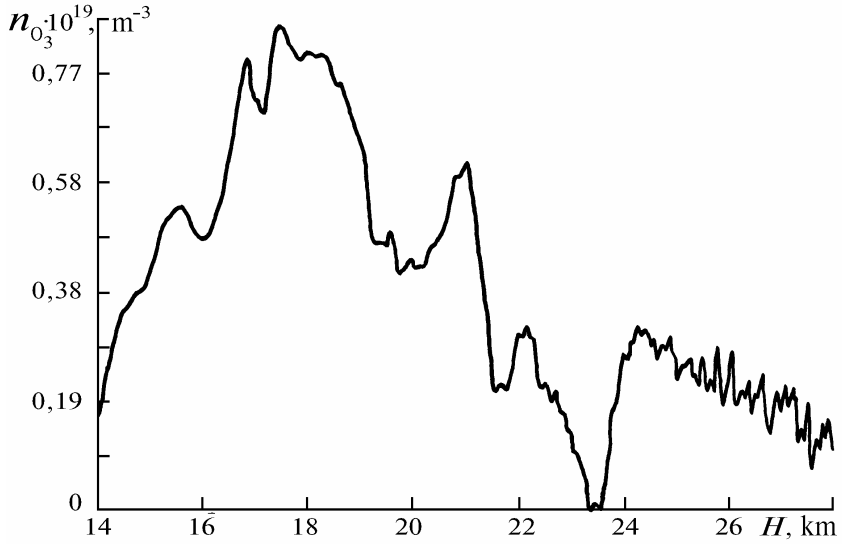

FIG. 24. The ozone concentration calculated from the two signals with vertical resolution of 1.5 km. *A correction was only made for the Rayleigh extinction.*

in December, 1991 and January, 1992 revealed its lower content as compared to the climatological mean at the Observatoire de Haute–Provence. It is rather difficult to establish a direct relation between stratospheric ozone concentration and the aerosol volcanic cloud. A more comprehensive study of the extension an temporal variability of the Pinatubo volcanic cloud in the mid– and high–latitude regions is still needed.

Nevertheless measurements carried out after the Mts. Agung and El Chichon eruptions showed negative correlation between ozone and volcanic stratospheric aerosol. Evidence for negative correlations between ozone and arctic aerosol was also found during polar winters. It was only after the discovery of the Antarctic ozone hole that catalytic effects related to heterogeneous chemistry and affecting the ozone content became the object of serious studies extended to investigation of the role of volcanic aerosol in the ozone reduction.

The measurements of ozone–aerosol correlation in the lower stratosphere were carried out within the framework of the European Stratospheric Ozone Experiment (EASOE) at Thule (Greenland, 76.5°N, 68.8°W) in winter 1991–1992, Ref. 12. The EASOE Campaign was aimed at monitoring ozone destruction observed in polar regions. During the campaign a large set of ground–based, balloon, and airborne instruments were deployed in the Arctic.

A lidar system in Thule is operated in a routine mode of aerosol observations since November 1990. It involves a transmitter based on a Nd:YAG laser (532 nm, 100 mJ, 4 Hz) and a receiving Cassegrainian telescope of a 800 mm diameter. In the same period, a large number (about 40) of ozone–sondes were launched.

During the aerosol (lidar) and ozone (ECC–sonde) measurements no formations of stratospheric polar clouds were observed. This is consistent with relatively high temperature in the stratosphere which was almost always above 200 K. However, at this same time, a large amount of aerosol was injected into the stratosphere by the Mt. Pinatubo eruption. To study correlations between ozone and aerosol the profiles of aerosol backscattering coefficient β_π, depolarization ratio and ozone concentration n_{O_3} were used.

In Fig. 25 the profiles of n_{O_3} and β_π are compared. The lidar profile was accumulated during the ECC–sonde ascent to the maximum height.

Cross correlation coefficients (the ozone and aerosol deviations from average values) were calculated in ± 2 km height intervals around a given level for 25 couples of β_π and n_{O_3} measurements. Sometimes, the value of the negative cross correlation coefficient reached 0.97 (February 24, height 17 km). The average coefficients were negative in the lower stratosphere and reached values around – 0.5 in the 13–18 km height range.

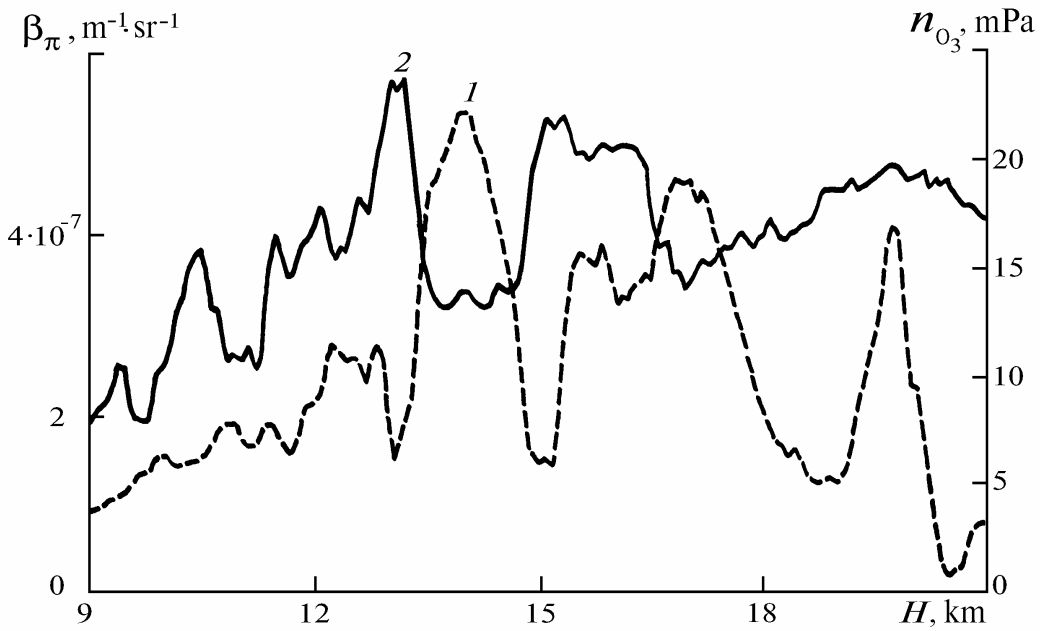

FIG. 25. Backscattering coefficient (curve 1) and ozone partial pressure (curve 2) over Thule on February 6, 1992.

A study of the air mass trajectories was carried out to establish possible formation of polar stratospheric clouds (PSC), however, it is not obvious that ozone destruction is caused by these clouds.

The processes of ozone destruction are planned to be examined at a new atmospheric observatory in the Canadian Arctic[13] (Eureka, Ellesmere Island, 80°N, 86°W). The observatory will be equipped with two lidars: a stratospheric ozone DIAL and a Polar Stratospheric Clouds/Arctic Haze Lidar. The receiving telescope of each lidar is enclosed inside a small compartment which is thermally insulated from the rest of the laboratory and is kept at the outside ambient temperature.

The ozone DIAL lidar will be capable of operating during daytime and will provide measurements of the stratospheric ozone concentration profiles through all year. It will also allow studies of the ozone layer interactions with solar radiation under the unique illumination conditions of this location to be carried out. The lidar consists of a XeCl excimer laser (60 W, 300 Hz) with a pressurized hydrogen Raman cell, a Newtonian telescope of 1 m aperture equipped with several special blocks to facilitate daytime operation.

The second lidar consists of a Nd:YAG laser (10 W, 20 Hz) emitting at 1.06 and 0.532 μm. Separate receivers are used for the PSC and haze measurements. Polarization measurement capabilities are available at both wavelengths. The Eureka observatory with the lidar facilities and other atmospheric sensors will be a part of the global Network for Detection of Stratospheric Change (NDSC). It will be put into operation in early 1993.

The study of the ozone layer in high–latitude regions was undertaken by the Campaign called EASOE (European Arctic Stratospheric Ozone Experiment) during the winter 1991–1992, Ref. 14. Its main objective was to establish a budget of the ozone destruction processes over the whole northern hemisphere. Different types of instruments located in both high– and mid–latitude regions were used. The lidar system was mounted in Sodankyla (Finland, 67°N, 27°E) and involved an ozone and multiwave aerosol lidars for measuring PSC. The first lidar was developed in IROE (Florence, Italy) and the second one at the university FREIE (Berlin, Germany).

Of particular interest is a mobile ozone lidar which makes it possible to obtain continuous ozone profiles in the altitude range between 5 to 40 km. The ozone lidar is a combination of two lidar systems. The "tropospheric" lidar transmitter involved two Nd:YAG lasers (Spectra–Physics) emitting respectively 40 mJ and 60 mJ per pulse at the fourth harmonic, at a repetition frequency 10 Hz (Fig. 26). The 289 and 299 nm wavelengths were generated by one of the lasers in SRS–cells filled with D_2 and H_2 and having energy of 8 and 10 mJ per pulse. The 355 nm wavelength was generated by the second laser at the third harmonic with energy 40–80 mJ/pulse. The transmitter of the "stratospheric" lidar used a XeCl excimer laser (LPX–200) (200 mJ/pulse, 80 Hz).

Unstable resonator optics was used to limit the beam divergence to 0.5 mrad which at the output passed through the collimators with 2.5 magnification factor for the Nd: YAG laser and 3 for the XeCl laser.

The optical receiving system was constructed of four similar mirrors of 50 cm diameter (Fig. 27). The light was collected by four optical fibbers of 1 mm diameter. The fibber mounts were motorized in the X–Y directions for the alignment of each mirror with respect to the different laser beams. Then the optical fibbers transmitted the backscattered light to the optical analyzing device which included an imaging optics, a mechanical chopper used only for stratospheric measurements, and a multichannel monochromator designed for the wavelength separation.

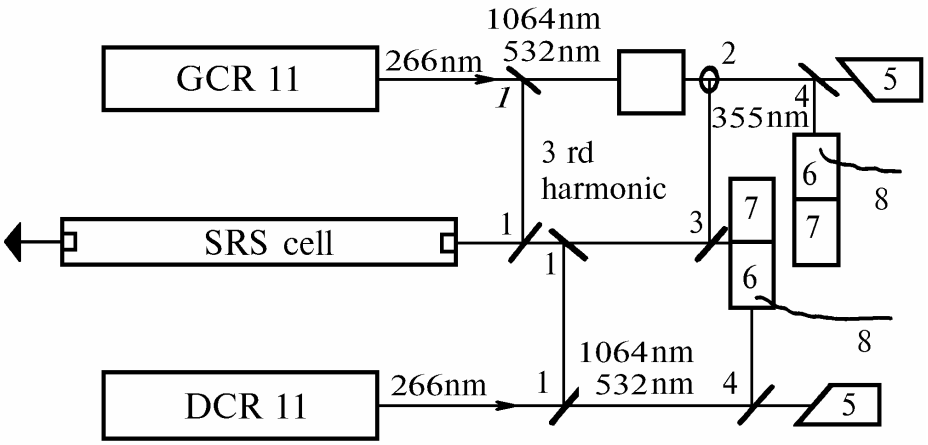

FIG. 26. Optical arrangement of the transmitter: dichroic mirrors for 4th harmonic (1), 3rd harmonic collimator (2), dichroic mirrors for 355 nm (3), *dichroic mirrors for* 532 nm (4), *optical Q–switch (5), attenuator for* 532 nm (6), *photodiodes for the 4th harmonic (7), and optical fibbers for synchronization (8).*

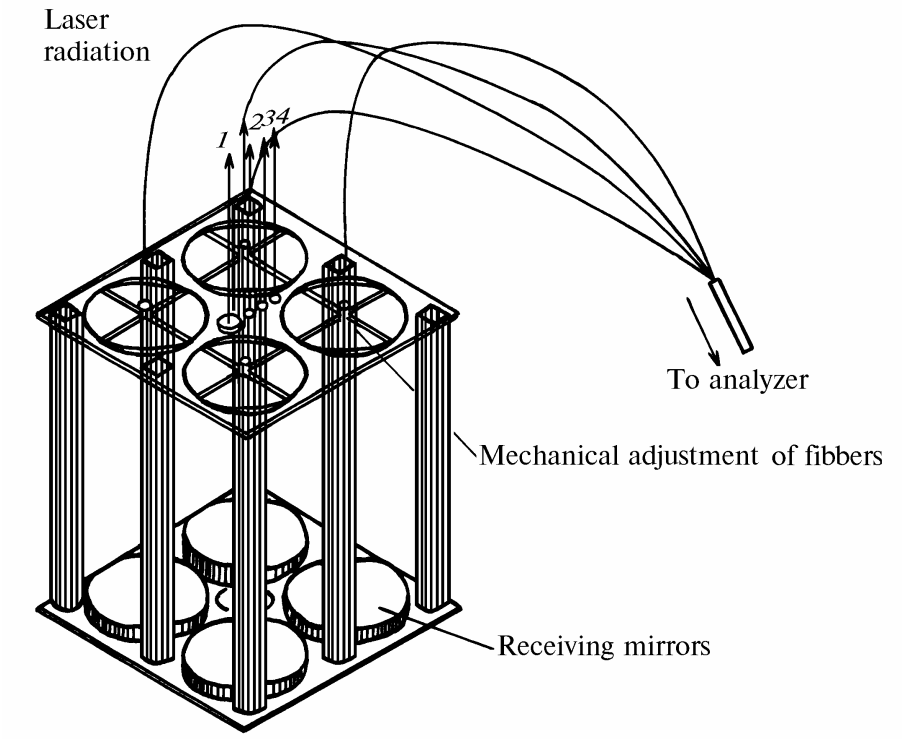

FIG. 27. Optical receiving system. Laser radiation at wavelengths: 308 nm (1), 289 (2), 299 (3), *and* 355 nm (4).

An electronic part of the lidar involved a synchronization system and a data acquisition system. The whole experiment was driven by a 386 PC computer which allowed simultaneous operation of two lasers and acquisition from 2 counting channels and 4 analog channels to be performed. The data acquisition system included four 10 MHz 12 bits waveform recorders for analog detection and two 200 MHz photoncounting units. Both detection modes could work simultaneously. During the acquisition, the computer provided real time plots as well as ozone profiles calculated on a limited number of shots in order to check the validity of the experiment.

REFERENCES

1. W.B. Grant, E.V. Browell, et al., Abstact of papers 16 ILRC, MIT, July 20–24, 1992, pp. 23–26.
2. A.Apituley, J. Bosenberg, et al., Ibid., pp. 53–55.
3. W. Steinbrecht and A.I. Carswell, Ibid., pp. 27–30.
4. W. Vandersee, F. Schonenborn, and H. Claude, ibid., pp. 109–111.
5. U.N. Singh, Th.J. McGee, et al., Ibid., pp. 31–33.
6. I.S. McDermid, Ibid., pp. 35–38.
7. H. Nakane, S. Hayashida, et al., Ibid., pp. 45–48.
8. Th. McGee, U.N. Singh, et al., Ibid., pp. 103–106.
9. M.A. Fenn, E.V. Browell et al., Ibid., pp. 117–120.
10. M. Wirth, W. Renger, and G.Eher, Ibid., pp. 107–108.
11. G. Megie, S. Godin, et al., Ibid., pp. 39–41.
12. P.Di. Girolano, M. Cacciani, et al., Ibid., pp. 49–51.
13. A. Ulitsky, T.Yu. Wang, et al., Ibid., pp. 43–44.
14. S. Godin, G. Ancellet, et al., Ibid., pp. 113–115.